Vibrational Energy Relaxation of Polyatomic Molecules in Liquid Solution via the Linearized Semiclassical Method

Being J. Ka and Eitan Geva*

Department of Chemistry, University of Michigan, Ann Arbor, Michigan 48109-1055

Received: April 17, 2006; In Final Form: June 2, 2006

Vibrational energy relaxation (VER) of polyatomic, as opposed to diatomic, molecules can occur via different, often solvent assisted, intramolecular and/or intermolecular pathways. In this paper, we apply the linearized semiclassical (LSC) method for calculating VER rates in the prototypical case of a rigid, symmetrical and linear triatomic molecule (A−B−A) in a monatomic liquid. Starting at the first excited state of either the symmetric or asymmetric stretches, VER can occur either directly to the ground state or indirectly via intramolecular vibrational relaxation (IVR). The VER rate constants for the various pathways are calculated within the framework of the Landau−Teller formalism, where they are expressed in terms of two-time quantum-mechanical correlation functions. The latter are calculated by the LHA−LSC method, which puts them in a "Wignerized" form, and employs a local harmonic approximation (LHA) in order to compute the necessary multidimensional Wigner integrals. Results are reported for the LHL/Ar model of Deng and Stratt [*J. Chem. Phys.* **2002**, *117*, 1735], as well as for CO_2 in liquid argon and in liquid neon. The LHA−LSC method is shown to give rise to significantly faster VER and IVR rates in comparison to the classical treatment, particularly at lower temperatures. We also find that the type and extent of the quantum rate enhancement is strongly dependent on the particular VER pathway. Finally, we find that the classical and semiclassical treatments can give rise to opposite trends when it comes to the dependence of the VER rates on the solvent.

I. Introduction

Vibrational energy relaxation (VER) is the fundamental process by which an excited vibrational mode releases its excess energy to other, intermolecular and/or intramolecular, degrees of freedom (DOF). Virtually all chemical phenomena in the condensed phase involve VER processes. The measurement and calculation of VER rates in such systems have therefore received much attention over the last few decades.[1−49] Recent theoretical and computational studies of VER have been mostly based on the Landau−Teller (LT) formula,[15,50] which is derived by assuming weak coupling between the relaxing mode and the accepting DOF and neglecting solvent induced fluctuations of the vibrational frequency.[47] This formulation puts the VER rate constant in terms of the Fourier transform (FT), at the vibrational frequency ω, of a certain quantum mechanical autocorrelation function of the force exerted on the relaxing mode by the remaining DOF. The fact that for most molecular vibrations $\hbar\omega/k_BT \gg 1$, even at room temperature, implies that replacing the quantum-mechanical force-force correlation function (FFCF) by its classical counterpart is in general not justified. Indeed, discrepancies by many orders of magnitude have been reported between experimentally measured VER rates and predictions based on classical molecular dynamics simulations.[51−55] At the same time, a numerically exact calculation of the quantum-mechanical FFCF in liquid solutions is not feasible. The most popular approach for dealing with this difficulty has been based on multiplying the classical prediction for the VER rate constant by a frequency-dependent quantum correction factor (QCF).[3,56−71] Many different approximate QCFs have been proposed in the literature. Unfortunately, the choice of QCF is often rather ad hoc and estimates obtained from different QCFs can differ by orders of magnitude, particularly when high-frequency vibrations are involved. The development of more rigorous methods for computing VER rate constants is therefore clearly highly desirable.

We have recently introduced a new approach for calculating VER rate constants, which is based on estimating the quantum-mechanical FFCF via the linearized semiclassical (LSC) approximation. The latter approximation involves linearizing the forward−backward path integral action in the exact quantum-mechanical FFCF, with respect to the difference between the forward and backward paths.[72] This leads to a classical-like expression for the FFCF, where the classical variables are replaced by certain Wigner transforms of the corresponding quantum-mechanical operators. We have also introduced a local harmonic approximation (LHA) in order to evaluate these Wigner transforms in many-body anharmonic systems.[53] In the remainder of this paper, we will refer to the method that results from the combination of the LSC and LHA approximations as LHA−LSC.

In previous work, we have demonstrated the accuracy of the LHA−LSC method on the following nontrivial benchmark problems:[53] (1) a vibrational mode coupled to a harmonic bath, with the coupling exponential in the bath coordinates, and (2) a diatomic coupled to a short linear chain of helium atoms. The feasibility of applying the method to molecular liquids was also demonstrated via applications to a "breathing sphere" diatomic in a two-dimensional monatomic liquid, as well as to neat liquid oxygen, neat liquid nitrogen, and liquid oxygen/argon mixtures.[53−55] We have also performed a systematic analysis of the temperature and mole fraction dependence of the LHA−LSC-based VER rates, as well as of the importance of different contributions to them.[55] The LHA−LSC-based predictions were found to be of the same order of magnitude as the experimental

* Corresponding author. E-mail: eitan@umich.edu.

10.1021/jp062363c CCC: $33.50
Published on Web 07/15/2006

results (when available). This represents a dramatic improvement in comparison to the classical predictions which are smaller than the experimental results by many orders of magnitude. We have also shown that the LHA−LSC method can accurately reproduce the experimental dependence of the VER rate on temperature in the case of neat liquid oxygen and the dependence of the VER rate on the oxygen mole fraction in the case of liquid oxygen/argon mixtures.[55] Our work has also shown that obtaining accurate predictions requires that one account for quantum delocalization and nonclassical sampling.[54,55]

In recent experimental studies of VER, attention has been shifting to polyatomic solute/solvent systems.[37,73−77] The main new feature of VER in polyatomic molecules, as opposed to diatomic molecules, has to do with the fact that it can occur via different intramolecular and/or intermolecular pathways. Indeed, VER in polyatomic molecules often involves solvent-assisted intramolecular vibrational relaxation (IVR).[43,78] More specifically, the solvent can induce coupling between intramolecular modes of a polyatomic solute, which would be uncoupled in the isolated molecule. The case of small polyatomic molecules (3−4 atoms) is particularly attractive since the modes that define the vibrational spectrum are more or less isolated, and the number of VER pathways is relatively small.

IR-pump/Raman-probe spectroscopy is arguably the most powerful experimental method available for studying VER pathways in polyatomic liquids.[18,79,80] In this technique, a short IR pulse is used to excite a vibrational mode, and a delayed visible probe generates anti-Stokes transients from all Raman active vibrations. This way, the relaxation of the pumped transition into first-generation daughters, and the subsequent decay into second- and even third-generation daughters, can be monitored in real time and with an unprecedented level of detail. This technique has been used for elucidating the VER pathway of high-frequency stretches in a variety of molecular liquids, including dichloromethane,[81] chloroform,[82,83] bromoform,[84] acetonitrile,[85,86] benzene,[87] nitromethane,[88] OClO in aqueous solution,[89] water and its isotopomers,[76,90−94] and alcohols.[90,95−97]

The wealth of detailed experimental information on VER in polyatomic solute/solvent systems has motivated many theoretical studies that attempted to provide a molecular interpretation of the observed time scales and pathways in such systems as a linear triatomic solute in a monatomic liquid,[43] OClO in water,[98] HOD in D_2O,[42,99,100] azide in water,[101,102] neat liquid chloroform,[45] and neat liquid methanol.[48,49] Those theoretical studies have been based on classical MD simulations, although a few have also attempted to account for quantum-mechanical effects through the use of QCFs.[42,43,60,100] Extending the range of application of the LHA−LSC method to such polyatomic liquid solutions is therefore highly desirable. In this paper, we take the first step in this direction by using the LHA−LSC method for calculating the rates of different VER pathways in the case of a rigid, symmetrical and linear triatomic molecule (A−B−A) in a monatomic liquid. In this case, VER from the first excited state of the symmetric or asymmetric stretches can occur either directly to the ground state or indirectly via IVR.

The remainder of this paper will be organized as follows. The model Hamiltonian of a symmetrical and linear triatomic solute in a monatomic liquid is outlined in section II. The general theoretical framework of VER in such systems is described in section III. The LHA−LSC method for calculating VER rates in this system is formulated in section IV. The three models on which calculations were performed are described in section V. The simulation techniques used for calculating the LHA−LSC-based VER rate constants are described in section VI. The simulation results are reported and analyzed in section VII. We conclude in section VIII with a summary of the main results and some discussion on their significance. Explicit mathematical expressions for quantities required for the evaluation of the LHA−LSC approximation are provided in the Appendix.

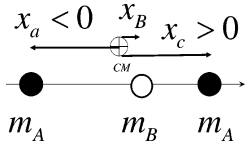

Figure 1. A schematic view of the linear symmetric triatomic molecule.

II. Model

The model that we will focus on in this paper probably corresponds to the simplest example of solvent-assisted VER involving a polyatomic solute. The polyatomic solute of choice corresponds to a *rigid*, linear and symmetric triatomic molecule, and the solvent is assumed to be monatomic. It should be noted that Deng and Stratt have recently employed a similar model for studying VER in a polyatomic molecule within the frameworks of classical mechanics, linearized instantaneous normal mode (INM) formalism (for IVR), and the instantaneous-pair theory (for intermolecular VER).[43]

The solvent-free Hamiltonian of the rigid, linear and symmetric solute molecule A−B−A is given by (cf. Figure 1)

$$H_s = \frac{p_a^2}{2m_A} + \frac{p_b^2}{2m_B} + \frac{p_c^2}{2m_A} + \frac{1}{2}\kappa(x_b - x_a - r_e)^2 + \frac{1}{2}\kappa(x_c - x_b - r_e)^2 \quad (1)$$

Here, $\{x_a, x_b, x_c\}$ and $\{p_a, p_b, p_c\}$ are the positions and corresponding momenta of the atomic sites *a*, *b*, and *c* relative to the molecular center of mass (projected along the molecular axis and such that $x_a < 0$ and $x_c > 0$); m_A and m_B are the masses of atoms A and B, respectively; κ is the spring constant; and r_e is the equilibrium A − B bond length. It should be noted that the bending modes were left out for the sake of simplicity. Accounting for stretch-to-bend VER pathways may be important in practice, and an extension of the methodology to include bending modes will be considered in future work. Furthermore, as pointed out by Deng and Stratt, symmetric to asymmetric IVR is actually not uncommon in polyatomic molecules.[43] We also note that the lack of anharmonic terms in the intramolecular potential implies that solvent-free IVR is neglected. This simplification reflects our desire to focus on *solvent-assisted* IVR.

We next rewrite the Hamiltonian in eq 1 in terms of the *symmetric* (s) stretch and *asymmetric* (as) stretch normal mode coordinates and momenta:

$$H_s = \frac{p_s^2}{2} + \frac{p_{as}^2}{2} + \frac{1}{2}\omega_s^2 q_s^2 + \frac{1}{2}\omega_{as}^2 q_{as}^2 \quad (2)$$

Here,

$$\omega_s = \sqrt{\kappa/m_A} \quad \text{and} \quad \omega_{as} = \sqrt{\kappa M/m_A m_B} \quad (3)$$

are the frequencies of the symmetric and asymmetric stretches, respectively, and $M = 2m_A + m_B$ is the molecular mass. It should be noted that

$$\frac{\omega_{as}}{\omega_s} = \sqrt{\frac{M}{m_B}} = \sqrt{1 + 2\frac{m_A}{m_B}} \quad (4)$$

such that $\omega_{as} > \omega_s$.

The corresponding normal mode coordinates are given by

$$\begin{pmatrix} q_s \\ q_{as} \end{pmatrix} = \begin{pmatrix} 1/\sqrt{2} & 0 & -1/\sqrt{2} \\ \sqrt{m_B/2M} & -\sqrt{2m_A/M} & \sqrt{m_B/2M} \end{pmatrix} \begin{pmatrix} q_a \\ q_b \\ q_c \end{pmatrix} \quad (5)$$

where $q_a = \sqrt{m_A}(x_a + r_e)$, $q_b = \sqrt{m_B}x_b$, and $q_c = \sqrt{m_A}(x_c - r_e)$ are the mass weighted displacements of the three atoms from their equilibrium positions. The reverse transformation from normal modes to local modes is given by

$$\begin{pmatrix} q_a \\ q_b \\ q_c \end{pmatrix} = \begin{pmatrix} 1/\sqrt{2} & \sqrt{m_B/2M} \\ 0 & -\sqrt{2m_A/M} \\ -1/\sqrt{2} & \sqrt{m_B/2M} \end{pmatrix} \begin{pmatrix} q_s \\ q_{as} \end{pmatrix} \quad (6)$$

Finally, we define a vector of atomic displacements, $\mathbf{q}$, which can be presented as either (q_a, q_b, q_c) or (q_s, q_{as}).

The translational and rotational kinetic energy terms of the free triatomic molecule are given by $\mathbf{P}_{CM}^2/2M$ and $\mathbf{L}^2/2I$, respectively, where $\mathbf{P}_{CM}$ is the molecular center of mass momentum, $\mathbf{L}$ is its overall angular momentum, and I is its moment of inertia (boldface symbols represent vectors throughout this paper):

$$\mathbf{P}_{CM} = \frac{m_A\mathbf{P}_a + m_B\mathbf{P}_b + m_A\mathbf{P}_c}{M} \quad (7)$$

$$\mathbf{L}^2 = r_e^2[(P_{a,x} - P_{c,x})^2 + (P_{a,y} - P_{c,y})^2 + (P_{a,z} - P_{c,z})^2] \quad (8)$$

$$I = m_A x_a^2 + m_B x_b^2 + m_A x_c^2 = (\sqrt{2m_A}r_e - q_s)^2 + q_{as}^2 \quad (9)$$

It should be noted that, unlike ref 43, we explicitly account for the vibrational−rotational coupling, which gives rise to VER via centrifugal forces. It should also be noted that a more *negative* q_s translates into *extension* along the A−B bonds, and therefore leads to a larger moment of inertia.

We next turn to the solvent, which we assume to be monatomic. The solvent−solvent interactions and the interactions between the solvent atoms and the three sites of the triatomic solute are described in terms of pair potentials, such that the overall solute + solvent Hamiltonian can be given in the following form:

$$H = H_s + T(\mathbf{q}) + U(\mathbf{q}) \quad (10)$$

Here,

$$T(\mathbf{q}) = \frac{\mathbf{P}_{CM}^2}{2M} + \frac{\mathbf{L}^2}{2I(\mathbf{q})} + \sum_{j=1}^{N}\frac{\mathbf{P}_j^2}{2m_S} \quad (11)$$

and

$$U(\mathbf{q}) = \sum_{\alpha=a,b,c}\sum_{j=1}^{N}\phi_\alpha\left(\left|\mathbf{r}_{j\alpha} + \frac{q_\alpha}{\sqrt{m_\alpha}}\Omega\right|\right) + \sum_{j=1}^{N-1}\sum_{k=j+1}^{N}\phi_s(r_{jk}) \quad (12)$$

where $\mathbf{P}_j$ is the momentum of the jth solvent atom, m_S is its mass, $\mathbf{r}_{j\alpha}$ is the vector pointing from the jth solvent atom to site α on the solute, Ω is a unit vector pointing from site a to site c of the triatomic molecule, and r_{jk} is the distance between the jth and kth solvent atoms.

The potential energy $U(\mathbf{q})$ in eq 12 involves three types of pair potentials corresponding to (1) the interaction between the solvent atoms, $\phi_s(r)$; (2) the interaction between atom A of the triatomic solute and the solvent atoms, $\phi_a(r) = \phi_c(r) \equiv \phi_A(r)$; and (3) the interaction between atom B of the triatomic solute and the solvent atoms, $\phi_b(r) \equiv \phi_B(r)$. In actual simulations, we have assumed that all of these pair potentials are of the Lennard-Jones (LJ) type, namely,

$$\phi_j(r) = 4\epsilon_j\left[\left(\frac{\sigma_j}{r}\right)^{12} - \left(\frac{\sigma_j}{r}\right)^{6}\right] \quad (13)$$

III. Vibrational Energy Relaxation Theory

The eigenfunctions of the solvent-free vibrational Hamiltonian H_s are given by $|n_s\rangle \otimes |n_{as}\rangle \equiv |n_s, n_{as}\rangle$, such that

$$H_s|n_s, n_{as}\rangle = (n_s\hbar\omega_s + n_{as}\hbar\omega_{as})|n_s, n_{as}\rangle \quad (14)$$

with $n_s, n_{as} = 0, 1, 2, \ldots$. VER proceeds via transitions between these solvent-free vibrational states. Within the framework of Fermi's golden rule, the rate constant for the transition from state $|n_s(i), n_{as}(i)\rangle$ to state $|n_s(f), n_{as}(f)\rangle$ is given by:

$$k_{f\leftarrow i} = \frac{1}{\hbar^2}\tilde{C}_{if}(\omega_{if}) \quad (15)$$

where

$$\tilde{C}_{if}(\omega_{if}) = \int_{-\infty}^{\infty} e^{i\omega_{if}t}C_{if}(t) = \frac{4}{1 + e^{-\beta\hbar\omega_{if}}}\int_0^\infty \cos[\omega_{if}t]\,\mathrm{Re}\{C_{if}(t)\} = -\frac{4}{1 - e^{-\beta\hbar\omega_{if}}}\int_0^\infty \sin[\omega_{if}t]\,\mathrm{Im}\{C_{if}(t)\} \quad (16)$$

and

$$C_{if}(t) = Z_b^{-1}\,\mathrm{Tr}\{e^{-\beta H_b}\,e^{iH_bt/\hbar}\langle n_s(i), n_{as}(i)|T(\mathbf{q}) + U(\mathbf{q})|n_s(f), n_{as}(f)\rangle e^{-iH_bt/\hbar}\langle n_s(i), n_{as}(i)|T(\mathbf{q}) + U(\mathbf{q})|n_s(f), n_{as}(f)\rangle\} \quad (17)$$

Here, $\omega_{if} = [n_s(f) - n_s(i)]\omega_s + [n_{as}(f) - n_{as}(i)]\omega_{as}$, $H_b = T(0) + U(0)$, $\beta = 1/k_BT$, and $Z_b = Tr\{e^{-\beta H_b}\}$.

In practice, the evaluation of $\langle n_s(i), n_{as}(i)|T(\mathbf{q}) + U(\mathbf{q})|n_s(f), n_{as}(f)\rangle$ is usually based on expanding $U(\mathbf{q})$ and $T(\mathbf{q})$ in powers of $\mathbf{q}$:

$$U(\mathbf{q}) = U(0) - (F_{U,s}, F_{U,as})\begin{pmatrix} q_s \\ q_{as} \end{pmatrix} + (q_s, q_{as})\begin{pmatrix} G_{U,s,s} & G_{U,s,as} \\ G_{U,as,s} & G_{U,as,as} \end{pmatrix}\begin{pmatrix} q_s \\ q_{as} \end{pmatrix} + \ldots \quad (18)$$

$$T(\mathbf{q}) = T(0) - (F_{T,s}, F_{T,as})\begin{pmatrix} q_s \\ q_{as} \end{pmatrix} + (q_s, q_{as})\begin{pmatrix} G_{T,s,s} & G_{T,s,as} \\ G_{T,as,s} & G_{T,as,as} \end{pmatrix}\begin{pmatrix} q_s \\ q_{as} \end{pmatrix} + \ldots \quad (19)$$

Substituting these expansions into $\langle n_s(i), n_{as}(i)|T(\mathbf{q}) + U(\mathbf{q})|n_s(f), n_{as}(f)\rangle$, one finds that $F_{U,s}$ and $F_{T,s}$ induce $(n_s, n_{as}) \rightarrow (n_s \pm 1, n_{as})$ transitions, $F_{U,as}$ and $F_{T,as}$ induce $(n_s, n_{as}) \rightarrow (n_s, n_{as} \pm 1)$ transitions, $G_{U,s,s}$ and $G_{T,s,s}$ induce $(n_s, n_{as}) \rightarrow (n_s \pm 2, n_{as})$ transitions, $G_{U,as,as}$ and $G_{T,as,as}$ induce $(n_s, n_{as}) \rightarrow (n_s, n_{as} \pm 2)$

transitions, and $G_{U,\mathrm{s,as}}$ and $G_{T,\mathrm{s,as}}$ induce $(n_\mathrm{s}, n_\mathrm{as}) \rightarrow (n_\mathrm{s} \pm 1, n_\mathrm{as} \mp 1)$ transitions. Thus, the lowest order contributions to *intermolecular* VER are associated with $F_{U,\mathrm{s}}$, $F_{U,\mathrm{as}}$, $F_{T,\mathrm{s}}$, and $F_{T,\mathrm{as}}$, while the lowest order contribution to IVR is associated with $G_{U,\mathrm{s,as}}$ and $G_{T,\mathrm{s,as}}$. We will also assume that the lowest order contributions are the dominant ones, such that contributions from higher order terms can be neglected (including those arising from $G_{U,\mathrm{s,s}}$, $G_{T,\mathrm{s,s}}$, $G_{U,\mathrm{as,as}}$, and $G_{T,\mathrm{as,as}}$).

The expansion coefficients $F_{U,\mathrm{s}}$, $F_{U,\mathrm{as}}$, $F_{T,\mathrm{s}}$, $F_{T,\mathrm{as}}$, $G_{U,\mathrm{s,as}}$, and $G_{T,\mathrm{s,as}}$ for the model under discussion are given by[43]

$$F_{U,\mathrm{s}} = \frac{1}{\sqrt{2m_\mathrm{A}}}(F_a - F_c)$$

$$F_{U,\mathrm{as}} = \frac{1}{\sqrt{2m_\mathrm{A}m_\mathrm{B}M}}(m_\mathrm{B}F_a - 2m_\mathrm{A}F_b + m_\mathrm{B}F_c)$$

$$G_{U,\mathrm{s,as}} = \frac{1}{\sqrt{2m_\mathrm{A}}}\sqrt{\frac{m_\mathrm{B}}{M}}(G_{aa} - G_{cc})$$

$$F_{T,\mathrm{s}} = -\frac{L^2}{2m_\mathrm{A}r_\mathrm{e}^3}, \quad F_{T,\mathrm{as}} = 0, \quad G_{T,\mathrm{s,as}} = 0 \tag{20}$$

where

$$F_\alpha = -\frac{\partial U}{\partial x_\alpha}\Big|_{\mathbf{q}=0} = -\sum_{j=1}^{N}\phi'_\alpha(r_{j\alpha})\frac{\mathbf{r}_{j\alpha}\cdot\Omega}{r_{j\alpha}}$$

$$G_{\alpha\alpha} = \frac{\partial^2 U}{\partial x_\alpha^2}\Big|_{\mathbf{q}=0} = \sum_{j=1}^{N}\left\{-\frac{\phi'_\alpha(r_{j\alpha})}{r_{j\alpha}} + \frac{(\mathbf{r}_{j\alpha}\cdot\Omega)^2}{r_{j\alpha}}\left[\phi''_\alpha(r_{j\alpha}) - \frac{\mathbf{r}_{j\alpha}\cdot\Omega}{r_{j\alpha}}\right]\right\} \tag{21}$$

It should be noted that the centrifugal coupling only contributes to the intermolecular VER of the symmetric mode.

Starting at the first excited state of the *asymmetric* stretch, $|n_\mathrm{s}(i), n_\mathrm{as}(i)\rangle = |0, 1\rangle$, VER can follow one of two pathways (cf. Figure 2).

1. VER to the $|0, 0\rangle$ state with the rate constant:

$$k_\mathrm{as} = \frac{1}{2\hbar\omega_\mathrm{as}}\int_{-\infty}^{\infty}\mathrm{d}t\, \mathrm{e}^{-i\omega_\mathrm{as}t}C_\mathrm{as}(t) \tag{22}$$

where

$$C_\mathrm{as}(t) = Z_b^{-1}Tr\{\mathrm{e}^{-\beta H_b}\mathrm{e}^{iH_bt/\hbar}F_{U,\mathrm{as}}\mathrm{e}^{-iH_bt/\hbar}F_{U,\mathrm{as}}\} \tag{23}$$

2. IVR to the $|1, 0\rangle$ state with the rate constant:

$$k_\mathrm{ivr} = \frac{1}{4\omega_\mathrm{as}\omega_\mathrm{s}}\int_{-\infty}^{\infty}\mathrm{d}t\, \mathrm{e}^{-i\omega_\mathrm{ivr}t}C_\mathrm{ivr}(t) \tag{24}$$

where $\omega_\mathrm{ivr} = \omega_\mathrm{as} - \omega_\mathrm{s}$, and

$$C_\mathrm{ivr}(t) = Z_b^{-1}Tr\{\mathrm{e}^{-\beta H_b}\mathrm{e}^{iH_bt/\hbar}G_{U,\mathrm{s,as}}\mathrm{e}^{-iH_bt/\hbar}G_{U,\mathrm{s,as}}\} \tag{25}$$

It should be noted that accounting for IVR between $|0, 1\rangle$ and $|2, 0\rangle$ would require the inclusion of third-order expansion terms of the form $q_\mathrm{s}^2 q_\mathrm{as}$ in eqs 18 and 19, and is therefore not allowed within our model (even if these states are close in energy).

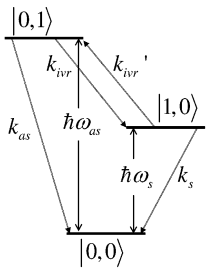

Figure 2. VER pathways in the linear symmetric triatomic molecule.

Next consider the possible VER pathways when one starts at the first excited state of the *symmetric* stretch, $|n_\mathrm{s}(i), n_\mathrm{as}(i)\rangle = |1, 0\rangle$. Here too, VER can follow one of two pathways (cf. Figure 2).

1. VER to the $|0, 0\rangle$ state with the rate constant:

$$k_\mathrm{s} = \frac{1}{2\hbar\omega_\mathrm{s}}\int_{-\infty}^{\infty}\mathrm{d}t\, \mathrm{e}^{-i\omega_\mathrm{s}t}C_\mathrm{s}(t) \tag{26}$$

where

$$C_\mathrm{s}(t) = Z_b^{-1}Tr\{\mathrm{e}^{-\beta H_b}\mathrm{e}^{iH_bt/\hbar}(F_{U,\mathrm{s}} + F_{T,\mathrm{s}})\mathrm{e}^{-iH_bt/\hbar}(F_{U,\mathrm{s}} + F_{T,\mathrm{s}})\} \tag{27}$$

2. IVR to the $|0, 1\rangle$ state with the rate constant:

$$k'_\mathrm{ivr} = \mathrm{e}^{-\beta\hbar\omega_\mathrm{ivr}}k_\mathrm{ivr} \tag{28}$$

It should be noted that significant IVR from the symmetric stretch to the asymmetric stretch requires that $\beta\hbar\omega_\mathrm{ivr}$ is comparable to or smaller than unity.

Finally, it should also be noted that transitions from the ground state $|0, 0\rangle$ to the first, $|1, 0\rangle$, and second, $|0, 1\rangle$, excited states can be assumed to be negligibly slow, given that $\beta\hbar\omega_\mathrm{s}$, $\beta\hbar\omega_\mathrm{as} \gg 1$.

IV. The linearized Semiclassical Approximation

In this section, we will outline the application of the LHA−LSC method for calculating the three quantum-mechanical correlation functions, $C_\mathrm{s}(t)$, $C_\mathrm{as}(t)$, and $C_\mathrm{ivr}(t)$ (cf. eqs 23, 27, and 25, respectively). In doing so, we will follow and extend procedures previously used for studying VER in the case of diatomic molecules in liquid solution.[54,55]

We will start out with the LSC approximation for $C_\mathrm{as}(t)$, which only involves the potential force $F_{U,\mathrm{as}}$. The LSC approximation for this correlation function is given by[53,54,72]

$$C_\mathrm{as}(t) \approx \frac{1}{Z_b}\frac{1}{(2\pi\hbar)^N}\int\mathrm{d}\mathbf{Q}_0\int\mathrm{d}\mathbf{P}_0[\delta F_{U,\mathrm{as}}\mathrm{e}^{-\beta H_b}]_W(\mathbf{Q}_0, \mathbf{P}_0) \times [\delta F_{U,\mathrm{as}}]_W(\mathbf{Q}_\mathrm{t}^{(\mathrm{Cl})}, \mathbf{P}_\mathrm{t}^{(\mathrm{Cl})}) \tag{29}$$

Here, $\mathbf{Q}_\mathrm{t}^{(\mathrm{Cl})} = \mathbf{Q}_\mathrm{t}^{(\mathrm{Cl})}(\mathbf{Q}_0, \mathbf{P}_0)$ and $\mathbf{P}_\mathrm{t}^{(\mathrm{Cl})} = \mathbf{P}_\mathrm{t}^{(\mathrm{Cl})}(\mathbf{Q}_0, \mathbf{P}_0)$ correspond to the Cartesian coordinates and momenta of all the atoms (including these that constitute the triatomic molecule), which are propagated classically with the initial conditions $\mathbf{Q}_0$ and $\mathbf{P}_0$, and

$$A_W(\mathbf{Q}, \mathbf{P}) = \int\mathrm{d}\mathbf{\Delta}\, \mathrm{e}^{-i\mathbf{P}\Delta/\hbar}\langle\mathbf{Q} + \mathbf{\Delta}/2|A|\mathbf{Q} - \mathbf{\Delta}/2\rangle \tag{30}$$

is the Wigner transform of the operator A.[103] The LHA is employed in order to calculate the Wigner transform $[\delta F_{U,\mathrm{as}}\mathrm{e}^{-\beta H_b}]_W(\mathbf{Q}_0, \mathbf{P}_0)$ in eq 29.[53−55] More specifically, we effectively

expand H_b and $F_{U,\mathrm{as}}$ to second order around $\mathbf{Q}_0$, followed by an analytical integration over $\mathbf{\Delta}$ of the Gaussian integral associated with $[\delta F_{U,\mathrm{as}} e^{-\beta H_b}]_W(\mathbf{Q}_0, \mathbf{P}_0)/\langle \mathbf{Q}_0|e^{-\beta H_b}|\mathbf{Q}_0\rangle$. This leads to the following LHA−LSC approximation for $C_{\mathrm{as}}(t)$:

$$C_{\mathrm{as}}(t) \approx \int d\mathbf{Q}_0 \frac{\langle \mathbf{Q}_0|e^{-\beta H_b}|\mathbf{Q}_0\rangle}{Z_b} \int d\mathbf{P}_{\mathrm{n},0} \prod_{j=1}^{N} \left(\frac{1}{\alpha^{(j)}\pi\hbar^2}\right)^{1/2} \exp\left[-\frac{(P_{\mathrm{n},0}^{(j)})^2}{\hbar^2\alpha^{(j)}}\right] [\delta F_{U,\mathrm{as}}(\mathbf{Q}_0) + D_{U,\mathrm{as}}(\mathbf{Q}_0, \mathbf{P}_{\mathrm{n},0})]\, \delta F_{U,\mathrm{as}}(\mathbf{Q}_{\mathrm{t}}^{(\mathrm{Cl})}) \tag{31}$$

Here, $\{P_{\mathrm{n}}^{(k)}\}$ are mass-wighted normal mode momenta, as obtained from the expansion of H_b to second order around $\mathbf{Q}_0$ (the LHA), and $\alpha^{(j)} = \mathbf{\Omega}^{(j)} \coth[\beta\hbar\mathbf{\Omega}^{(j)}/2]/\hbar$, where $\{(\mathbf{\Omega}^{(k)})^2\}$ are the eigenvalues of the corresponding Hessian matrix (explicit expressions of the potential derivatives underlying the LHA for the model considered here are provided in the Appendix). The term $D_{U,\mathrm{as}}(\mathbf{Q}_0, \mathbf{P}_{\mathrm{n},0})$ represents quantum nonlocality and is purely quantum-mechanical [i.e., it vanishes at the classical ($\hbar \to 0$) limit]. The explicit expression for this term can be found in ref 54, and some detailed expressions of quantities required in its evaluation for the model under discussion are provided in the Appendix. Another quantum-mechanical effect is introduced by the fact that the initial sampling of the positions and momenta is nonclassical. More specifically, the initial sampling of the positions is based on the exact quantum-mechanical position probability density, $\langle \mathbf{Q}_0|e^{-\beta H_b}|\mathbf{Q}_0\rangle/Z_b$, while the initial sampling of the momenta is based on the nonclassical probability density $\prod_{j=1}^{N}[1/(\alpha^{(j)}\pi\hbar^2)]^{1/2} \exp[-(P_{\mathrm{n},0}^{(j)})^2/(\hbar^2\alpha^{(j)})]$.

Next consider the correlation function $C_{\mathrm{s}}(t)$, which involves contributions from the potential force, $F_{U,\mathrm{s}}$, and centrifugal force, $F_{T,\mathrm{s}}$. The LHA−LSC approximation in this case can be obtained following the procedures previously developed for diatomic molecules, which lead to the following result:[54,55]

$$C_{\mathrm{s}}(t) \approx \int d\mathbf{Q}_0 \frac{\langle \mathbf{Q}_0|e^{-\beta H_b}|\mathbf{Q}_0\rangle}{Z_b} \int d\mathbf{P}_{\mathrm{n},0} \prod_{j=1}^{N} \left(\frac{1}{\alpha^{(j)}\pi\hbar^2}\right)^{1/2} \exp\left[-\frac{(P_{\mathrm{n},0}^{(j)})^2}{\hbar^2\alpha^{(j)}}\right] [\delta F_{U,\mathrm{s}}(\mathbf{Q}_0) + \delta F_{T,\mathrm{s}}(\mathbf{P}_0) + D_{U,\mathrm{s}}(\mathbf{Q}_0, \mathbf{P}_{\mathrm{n},0}) + D_{T,\mathrm{s}}(\mathbf{Q}_0, \mathbf{P}_{\mathrm{n},0})][\delta F_{U,\mathrm{s}}(\mathbf{Q}_{\mathrm{t}}^{(\mathrm{Cl})}) + \delta F_{T,\mathrm{s}}(\mathbf{Q}_{\mathrm{t}}^{(\mathrm{Cl})})] \tag{32}$$

$D_{T,\mathrm{s}}(\mathbf{Q}_0, \mathbf{P}_{\mathrm{n},0})$ and $D_{U,\mathrm{s}}(\mathbf{Q}_0, \mathbf{P}_{\mathrm{n},0})$ are purely quantum-mechanical nonlocal terms that originate from the centrifugal and potential forces, respectively. Explicit expressions for those terms can be found in ref 54, and some detailed expressions of quantities required for their evaluation (for the model under discussion) are provided in the Appendix.

We finally turn to the case of $C_{\mathrm{ivr}}(t)$. The latter is similar to $C_{\mathrm{as}}(t)$, and the only difference is that $F_{U,\mathrm{as}}$ is replaced by $G_{U,\mathrm{s,as}}$. Thus, the LHA−LSC approximation for $C_{\mathrm{ivr}}(t)$ is as follows:

$$C_{\mathrm{ivr}}(t) \approx \int d\mathbf{Q}_0 \frac{\langle \mathbf{Q}_0|e^{-\beta H_b}|\mathbf{Q}_0\rangle}{Z_b} \int d\mathbf{P}_{\mathrm{n},0} \prod_{j=1}^{N} \left(\frac{1}{\alpha^{(j)}\pi\hbar^2}\right)^{1/2} \exp\left[-\frac{(P_{\mathrm{n},0}^{(j)})^2}{\hbar^2\alpha^{(j)}}\right] [\delta G_{U,\mathrm{s,as}}(\mathbf{Q}_0) + D_{U,\mathrm{s,as}}(\mathbf{Q}_0, \mathbf{P}_{\mathrm{n},0})]\, \delta G_{U,\mathrm{s,as}}(\mathbf{Q}_{\mathrm{t}}^{(\mathrm{Cl})}) \tag{33}$$

TABLE 1: Model and Simulation Parameters[a]

model	LHL/Ar	CO_2/Ar	CO_2/Ne
r_e (Å)	1.1388	1.16	1.16
m_A (amu)	3.895	16.0	16.0
m_B (amu)	72.11	12.0	12.0
$\omega_{as}/2\pi c$ (cm^{-1})	2000	2400	2400
$\omega_s/2\pi c$ (cm^{-1})	1900	1253	1253
$\omega_{ivr}/2\pi c$ (cm^{-1})	100	1147	1147
ϵ_s/k_B (K)	117.7	117.7	47.0
σ_s (Å)	3.504	3.504	2.72
ϵ_A/k_B (K)	117.7	85.1	53.8
σ_A (Å)	3.504	3.23	2.84
ϵ_B/k_B (K)	117.7	77.6	49.1
σ_B (Å)	3.504	3.43	3.04
T (K)	294.25	94.16	37.6
ρ (nm^{-3})	24.4	19.76	42.24
time step (fs)	2.0	4.0	3.0

[a] All simulations were performed with one triatomic solute and 105 solvent atoms in the simulation box.

The purely quantum-mechanical term $D_{U,\mathrm{s,as}}(\mathbf{Q}_0, \mathbf{P}_{\mathrm{n},0})$ originates from the $G_{U,\mathrm{s,as}}$ coupling term which leads to IVR. An explicit expression for this term can be obtained by replacing $F_{U,\mathrm{as}}$ by $G_{U,\mathrm{s,as}}$ in the expression for $D_{U,\mathrm{as}}$. Some detailed expressions of quantities required for the evaluation of this term for the model under discussion are provided in the Appendix.

V. Model Parameters

Classical and LHA−LSC-based calculations of k_{s}, k_{as}, and k_{ivr} were performed on three different model systems and under different conditions as described below (cf. Table 1 for model parameters).

The first model that we considered is the LHL/Ar model, which was recently studied by Deng and Stratt within the classical INM formalism (for IVR) and instantaneous-pair theory (for intermolecular VER).[43] This model corresponds to the case where atom A is much lighter than atom B, such that $\omega_{\mathrm{as}} \sim \omega_{\mathrm{s}}$. More specifically, $m_A/m_B = 0.054$, which implies that $\omega_{\mathrm{as}}/\omega_{\mathrm{s}} = 1.053$. Unlike other models considered in ref 43, the frequencies assigned to the asymmetric and symmetric stretches were relatively high in this case, namely, $\omega_{\mathrm{as}}/2\pi c = 2000\ \mathrm{cm}^{-1}$ and $\omega_s/2\pi c = 1900\ \mathrm{cm}^{-1}$. The solvent corresponds to high-density supercritical argon fluid at room temperature ($\rho = 24.4\ \mathrm{nm}^{-3}$, $T = 294.25$ K). Since $\beta\hbar\omega_{\mathrm{as}} = 9.8$, $\beta\hbar\omega_{\mathrm{s}} = 9.3$, and $\beta\hbar\omega_{\mathrm{ivr}} = 0.49$, one expects sizable quantum corrections in the case of k_{as} and k_{s}, while a classical treatment is expected to provide relatively reliable results in the case of k_{ivr}. One also expects that, in this case, $k_{\mathrm{ivr}} \gg k_{\mathrm{as}}, k_{\mathrm{s}}$. If so, an equilibrium will be established between the symmetric and asymmetric excited states, prior to VER from either one of them to the ground state. Another interesting feature of this model has to do with the relatively small moment of inertia of the solute molecule, which suggests that centrifugal forces may contribute significantly to VER.

The second model consists of a CO_2-like solute in liquid argon ($\rho = 19.76\ \mathrm{nm}^{-3}$, $T = 94.16$ K). In this case, $\beta\hbar\omega_{\mathrm{as}} = 36.7$, $\beta\hbar\omega_{\mathrm{s}} = 19.2$, and $\beta\hbar\omega_{\mathrm{ivr}} = 17.5$. Thus, one expects more pronounced quantum corrections in this case, including for k_{ivr}. The relatively large value of $\beta\hbar\omega_{\mathrm{ivr}}$ also implies that IVR from the $|0, 1\rangle$ state to the $|1, 0\rangle$ state is an irreversible process. Thus, an excited symmetric stretch must relax to the ground state via the k_{s} pathway, while the excited asymmetric stretch can relax via either the k_{ivr} or k_{as} pathways.

The third model is similar to the second one, except for the fact that the solvent was changed from argon into neon. The same thermodynamic point in terms of reduced LJ units was

used ($T^* = 0.8$ and $\rho^* = 0.85$), such that the actual density and absolute temperature are $\rho = 42.24$ nm^{-3} and $T = 37.6$ K, respectively. As a result, $\beta\hbar\omega_{as} = 91.9$, $\beta\hbar\omega_s = 48.0$, and $\beta\hbar\omega_{ivr} = 43.9$. Hence, one expects the most pronounced quantum effects in this case.

VI. Simulation Techniques

Classical simulations on the LHL/Ar model were initiated with an overall number of 108 solvent atoms in a cubical simulation cell with standard periodic boundary conditions, which were organized in 27 unit cells (4 solvent atoms per unit cell). Three neighboring solvent atoms in a linear configuration were then replaced by the LHL molecule. The system was then equilibrated at a desired temperature for 20 ns with the help of the velocity rescaling method and the velocity Verlet algorithm.[104] The constraints imposed by the rigidity of the molecule were imposed explicitly by working in terms of the center of mass and angular momentum, rather than the Cartesian coordinates of the individual atoms. The equilibration period was followed by a calculation of the correlations functions $C_s(t)$, $C_{as}(t)$, and $C_{ivr}(t)$ by averaging over 10 240 equilibrium trajectories, each with 5000 time steps. Once the correlation functions were obtained, their FT was calculated via the FFT method. All of the results reported below were based on the cosine transform of the real part of the correlation functions.[55] In the case of very high vibrational frequencies (>500 cm^{-1}) the FT is a very small number and, therefore, very difficult to compute directly. Following the common practice, we instead extrapolated the exponential gap law, which was observed to emerge at low frequencies, to higher frequencies.[105,106] Assuming that this extrapolation is the major source of error in these cases, we evaluated the error bars reported for the VER rate constants based on the least-squares fit to the corresponding linear frequency dependence of the VER rate constant (on a semilog scale).

Classical simulations on the CO_2/Ar system were started by replacing the LHL molecule by a CO_2 molecule in an equilibrium configuration of the LHL/Ar system. The density was then modified to $\rho = 19.76$ nm^{-3} by changing the volume of the simulation cell, and the system was allowed to equilibrate for about 10 ns at $T = 94.16$ K. Classical simulations on the CO_2/Ne system were started with an equilibrium configuration of the CO_2/Ar system, where the argon atoms were replaced by neon atoms. The density was then modified to $\rho = 42.24$ nm^{-3} by changing the volume of the simulation cell, and the system was allowed to equilibrate for about 10 ns at $T = 37.6$ K. The subsequent calculation of the correlation functions $C_s(t)$, $C_{as}(t)$, and $C_{ivr}(t)$ and corresponding VER rate constants followed the same procedure as in the LHL/Ar system.

LHA−LSC-based calculations of k_s, k_{as}, and k_{ivr} followed a procedure similar to that previously described in the context of diatomic molecules.[55] The main difference between the current and previous studies is that, rather than restricting the LHA−LSC treatment to contributions from the first few solvation shells around the triatomic solute, we were able to apply it to all the atoms in the simulation cell (which was made possible by the availability of improved computer resources). The calculation starts by sampling the initial positions of all the atoms in the simulation cell via a PIMD simulation, where 16 beads were assigned to each atom. The PIMD simulation was started with all 16 beads in the position of the corresponding atom in a classical equilibrium configuration (as obtained from the classical simulation described in the previous paragraphs). This was followed by an equilibration period of 3 ps at the desired temperature, with the help of Nose-Hoover chain thermostats of length four (one thermostat for each of the three Cartesian coordinates of each atom), and the velocity Verlet algorithm.[107] It should be noted that the initial configurations sampled satisfied the constraint imposed by the linearity of the triatomic molecule.[54] The sampling was performed by choosing random beads from snapshots of the isomorphic liquid of cyclic polymers at each time step. An overall number of up to 286 000 initial configurations was used. For each of these, we calculated the normal mode frequencies and transformation matrix via the Jacobi method,[108] and used them in order to sample the initial normal mode momenta. Here too, we restrict ourselves to normal mode displacements which satisfy the constraints imposed by the linearity of the triatomic molecule.[54] We then performed a classical MD simulation over 500 time steps for each of the initial configurations, and extracted the correlation functions $C_s(t)$, $C_{as}(t)$, and $C_{ivr}(t)$ from them. It should be noted that, in calculating correlations functions via LHA−LSC, we can only correlate the relevant quantities at $t = 0$ and at a later time t.

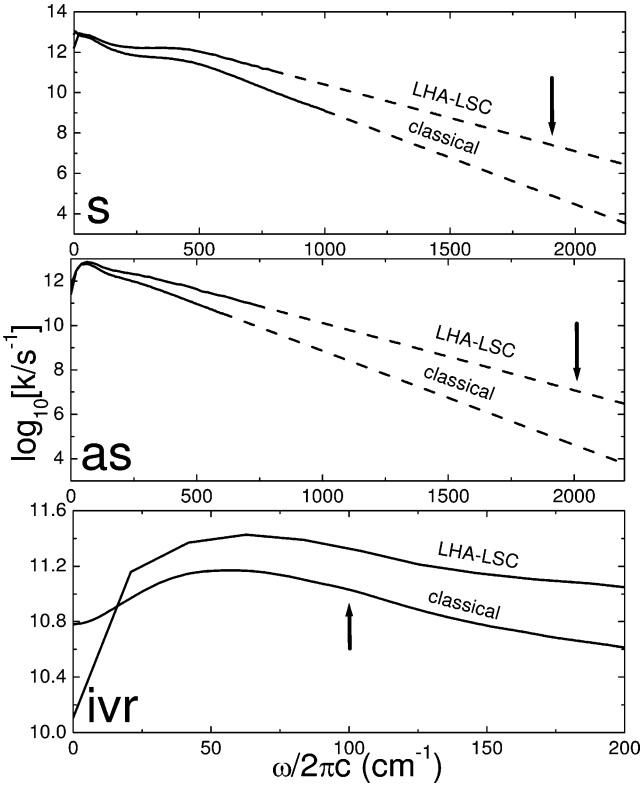

Figure 3. The classical and LHA−LSC frequency-dependent rate constants for the symmetric stretch, asymmetric stretch, and IVR, for LHL in argon. Calculated data are shown as solid lines. The dashed lines represent extrapolations to the corresponding frequencies of the symmetric and asymmetric stretches. The relevant frequencies are indicated by arrows.

VII. Results and Discussion

A. LHL in Liquid Argon at $\rho = 24.4$ nm^{-3} and $T = 294.25$ K. The VER rate constants k_{as}, k_s, and k_{ivr} for the LHL/Ar system are shown in Figure 3, as a function of frequency (on a semilog plot). The results obtained via the LHA−LSC method and fully classical calculations are shown. The corresponding values of k_{as}, k_s, and k_{ivr} at the actual frequencies ω_{as}, ω_s, and ω_{ivr} of the LHL molecule are reported in Table 2. Also given in this table are the values predicted by only using nonclassical initial sampling, while neglecting the nonlocal terms $D_{U,s}$, $D_{U,as}$, $D_{U,s,as}$, and $D_{T,s}$ (cf. eqs 31, 32, and 33).

TABLE 2: k_{as}, k_s, and k_{ivr} in the LHL/Ar System, as Obtained via the LHA−LSC Method[a]

LHL/Ar	$k_{as}/\mu s^{-1}$ U	$k_s/\mu s^{-1}$ U	$k_s/\mu s^{-1}$ U+T	k_{ivr}/ns^{-1} U	branching ratio $e^{\beta\hbar\omega_{ivr}}k_s/k_{as}$
classical	$(41 \pm 2) \times 10^{-3}$	$(70 \pm 10) \times 10^{-3}$	$(91 \pm 8) \times 10^{-3}$	109 ± 6	3.6 ± 0.5
nonclassical sampling	5 ± 1	16 ± 6	15 ± 5	$(2.0 \pm 0.5) \times 10^2$	5 ± 3
LHA−LSC	11 ± 3	28 ± 9	27 ± 8	$(2.0 \pm 0.5) \times 10^2$	4 ± 2
$f_{LHA-LSC}$	2.7×10^2	3.8×10^2	3.0×10^2	1.94	
f_{St}	2.0	2.0	2.0	1.24	
f_H	9.8	9.3	9.3	1.26	
f_{Sc}	133	104	104	1.28	
f_{MHS}	36	31	31	1.27	

[a] Also shown are the corresponding predictions obtained via fully classical simulations, and by using nonclassical initial sampling and neglecting the nonlocal terms. The branching ratio between the two possible VER pathways is shown in the right column. Also reported are the LHA−LSC-based quantum enhancement factor ($f_{LHA-LSC}$) and the following QCFs ($x = \beta\hbar\omega$): (1) standard $f_{St}(x) = 2/(1 + e^{-x})$, (2) harmonic $f_H(x) = x/(1 - e^{-x})$, (3) Schofield $f_{Sc} = e^x/2$, (4) mixed harmonic/Schofield $f_{MHS}(x) = \sqrt{xe^{x/2}/(1-e^{-x})}$.

We first note that our classical predictions for k_{as} and k_s are about 1 order of magnitude smaller than these reported by Deng and Stratt for the same model.[43] This discrepancy may be attributed to the fact that the values reported in ref 43 were obtained within the framework of the instantaneous pair theory, while the values reported in Table 2 were obtained by assuming that the exponential gap law observed at low frequencies can be extrapolated to higher frequencies. We also note that our prediction for the classical k_{ivr} is in excellent agreement with that reported in ref 43 (a numerically exact calculation of k_{ivr} is possible in this case due to the relatively small value of ω_{ivr}).

The classical k_s is about twice as large as k_{as}. A similar trend was also reported in ref 43, where it has been attributed to the fact that the solvent is more effective at relaxing the symmetric stretch. More specifically, the central B atom is protected from the solvent by the two terminal A atoms. The solvent is therefore ineffective in applying a force on the central B atom along the molecular axis. This implies that $F_{U,as} \approx \sqrt{m_B/(2m_AM)}(F_a + F_c)$, while $F_{U,s} = 1/\sqrt{2m_A}(F_a - F_c)$ (cf. eq 20). At the same time, F_a and F_c tend to have opposite signs because of the solvent's tendency to apply inward pressure. Thus, $|F_a - F_c| > |F_a + F_c|$, which implies that the solvent will be more effective at relaxing the symmetric stretch (to this end, also note that $m_B/M \sim 1$ in the case of the LHL model). In addition, it should be noted that $\omega_s < \omega_{as}$ makes the VER of the symmetric stretch even more effective because of the decrease in the density of accepting modes as the frequency increases.

The classical value of k_{ivr} is observed to be larger than k_s and k_{as} by about 6 orders of magnitude. The fact that $\beta\hbar\omega_{ivr} = 0.49$ also implies that $k'_{ivr} \sim k_{ivr} \gg k_s, k_{as}$. Thus, one expects an equilibrium to be established between the symmetric and asymmetric excited states, prior to VER from either one of these excited states to the ground state. The corresponding branching ratio is 3.6, which implies that about one out of four molecules will relax to the ground state via the asymmetric stretch. It should be noted that the fact that IVR is faster is a direct consequence of the small value of $\beta\hbar\omega_{ivr}$. In fact, the solvent is expected to be rather ineffective at assisting IVR.[43] This is because the potential curvatures G_{aa} and G_{cc} tend to have the same sign, such that $G_{U,s,as} \propto (G_{aa} - G_{cc})$ becomes small.

The frequency dependence of the LHA−LSC-based k_{as}, k_s, and k_{ivr} follows a trend which is similar to that observed in the classical case (cf. Figure 3). However, the actual values of k_{as}, k_s, and k_{ivr} obtained via the LHA−LSC method are generally larger than the classical ones (except at very low frequencies). The enhancement is much more pronounced in the case of k_s and k_{as}. More specifically, while k_{ivr} increases by a factor of about 2, k_s and k_{as} increase by 2 orders of magnitude. It is also interesting to note that the enhancement of the LHA−LSC-based k_s, k_{as}, and k_{ivr} is significantly larger than that predicted by various QCFs (cf. Table 2). Furthermore, LHA−LSC predicts a larger enhancement in the case of k_s, despite the fact that $\omega_s < \omega_{as}$. This should be contrasted with the commonly used QCFs, where the quantum enhancement of the VER rate constant is a monotonically increasing function of the frequency. The larger enhancement in the case of the symmetric stretch may reflect the fact that the solvent is more effective at relaxing it.[43]

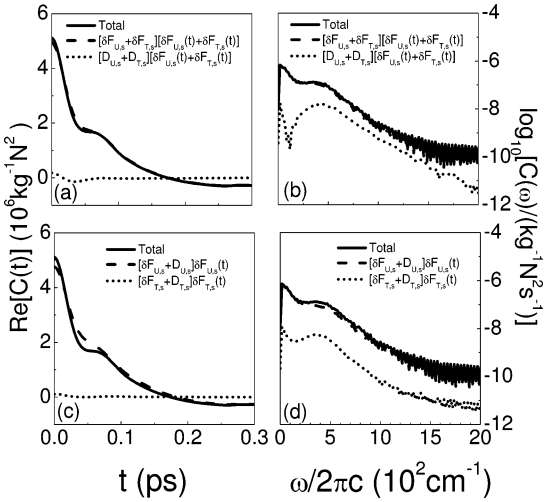

Figure 4. The force-force correlation function (a, c) and its Fourier transform (b, d), for the symmetrical stretch of LHL/Ar. Also shown are the relative contributions of the classical-like and quantum nonlocal terms (a, b), and the centrifugal and potential forces (c, d).

k_{ivr} is still about 4 orders of magnitude larger than k_s and k_{as} within the LHA−LSC treatment, which implies that equilibrium will still be established between the symmetric and asymmetric excited states, prior to VER to the ground state. The branching ratio is also similar to that in the classical case.

In Figure 4, we show the FFCF in the time and frequency domains (the latter is shown on a semilog plot), as obtained via the LHA−LSC method, for the symmetric stretch. Figure 4a shows the contributions to the FFCF from the classical-like term $[F_{U,s} + F_{T,s}][F_{U,s}(t) + F_{T,s}(t)]$ and nonclassical term $[D_{U,s} + D_{T,s}][F_{U,s}(t) + F_{T,s}(t)]$ (the initial sampling is nonclassical in both cases). The contributions of those two terms to the FT of the FFCF are shown in Figure 4b. The classical-like term is observed to dominate the FFCF in the time and frequency domains. Indeed, adding the nonclassical term is observed to increase k_s only by a factor of 2 (which should be contrasted to the overall enhancement of the LHA−LSC rate over the classical one by a factor of about 300). This observation should also be

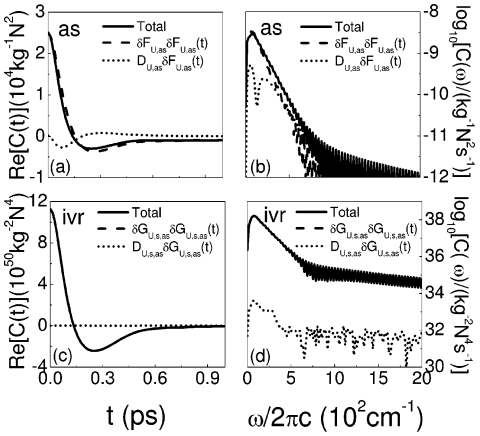

Figure 5. The force-force correlation function and its Fourier transform, for the asymmetric stretch (a, b) and IVR (c, d) of LHL/Ar. Also shown are the relative contributions of the classical-like and quantum nonlocal terms.

contrasted with previous applications of the LHA−LSC method to such systems as neat liquid oxygen, neat liquid nitrogen, and oxygen/argon mixtures,[55] where the nonclassical term was seen to dominate the high-frequency tail of the FFCF. However, it should be noted that $\beta\hbar\omega$ in the case of the LHL/Ar system is smaller by a factor of 4 or so in comparison to these other systems.

Figure 4c shows the contributions to the FFCF from the terms $[F_{T,s} + D_{T,s}]F_{T,s}(t)$ and $[F_{U,s} + D_{U,s}]F_{U,s}(t)$, which arise from the centrifugal and potential forces, respectively (cross terms are not shown explicitly, but can be deduced from the difference between the overall FFCF and the diagonal contributions). The corresponding contributions in the frequency domain are shown in Figure 4d. Despite the relatively large moment of inertia, the VER rate is clearly dominated by the potential force in both the time and frequency domains. In fact, unlike in the classical case, the effect of the centrifugal force, if any, falls within the error bar.

In Figure 5, we show the FFCF in the time and frequency domains (the latter is shown on a semilog plot), as obtained via the LHA−LSC method, for the asymmetric stretch and IVR. As for the symmetric stretch, the contribution of the nonclassical term to the overall quantum enhancement of k_{as} is relatively small (cf. Table 2). In the case of k_{ivr}, the nonclassical term does not even have an observable affect on k_{ivr}, which is consistent with the relatively small value of $\beta\hbar\omega_{ivr}$.

B. CO_2 in Liquid Argon at $\rho = 19.76$ nm^{-}3 and $T = 94.16$ K. The VER rate constants k_{as}, k_s, and k_{ivr} for the CO_2/Ar system are shown in Figure 6, as a function of frequency (on a semilog plot). The results obtained via the LHA−LSC method and fully classical calculations are shown. The values of k_{as}, k_s, and k_{ivr} at the actual frequencies ω_{as}, ω_s, and ω_{ivr} of the CO_2 are given in Table 3. Also given in this table are the values predicted by only using nonclassical initial sampling, while neglecting the nonlocal terms.

The classical rate for direct VER of the asymmetric stretch is extremely slow in this system ($k_{as} \sim 10^{-15}$ s^{-1}), which can be attributed to the relatively high value of $\beta\hbar\omega_{as}$ (∼37) and the fact that the bath is less effective at relaxing the asymmetric stretch.[43] k_{as} also remains negligibly slow within the LHA−LSC treatment, despite the enhancement by about 8 orders of magnitude relative to the classical result. Thus, the possibility of direct VER of the asymmetric stretch to the ground state can be ruled out.

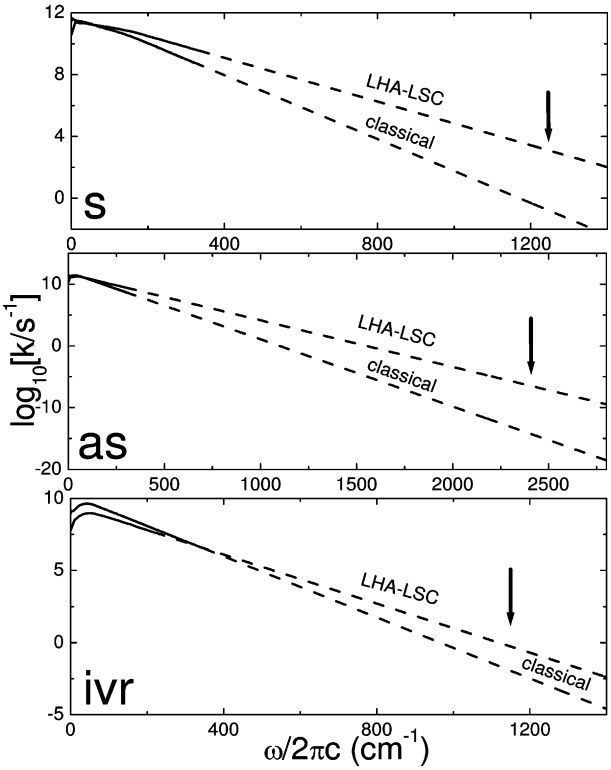

Figure 6. The classical and LHA−LSC frequency-dependent rate constants for the symmetric stretch, asymmetric stretch, and IVR, for CO_2 in argon. Calculated data are shown as solid lines. The dashed lines represent extrapolations to the corresponding frequencies of the symmetric and asymmetric stretches. The relevant frequencies are indicated by arrows.

The fastest VER rate in this system corresponds to k_s. In this case, the LHA−LSC method predicts $k_s \sim 10^3$ s^{-1}, which represents a quantum enhancement by about 4 orders of magnitude relative to the corresponding classical result (∼10^{-1} s^{-1}). For IVR, the LHA−LSC method predicts $k_{ivr} \sim 0.6$ s^{-1}, which is faster than the corresponding classical result by a factor of about 50. Given that $\beta\hbar\omega_s \sim \beta\hbar\omega_{ivr}$, this difference can only be attributed to the fact that the solvent is more effective at assisting VER of the symmetric stretch than IVR.[43] Furthermore, since $\beta\hbar\omega_s$, $\beta\hbar\omega_{ivr} \gg 1$, the corresponding reverse processes are negligibly slow. Thus, the rate of VER from the excited asymmetric stretch is dictated by k_{ivr}, while that from the excited symmetric stretch is dictated by by k_s (and is therefore significantly faster).

The relative roles of nonclassical sampling and the nonclassical term can also be inferred from the results presented in Table 3. More specifically, while the addition of the nonclassical term enhances k_s and k_{as} by 1 and 2 orders of magnitude, respectively, it has no noticeable effect on k_{ivr}. As for the LHL/Ar model, it is also found that the contribution of the centrifugal force to k_s is negligible. Finally, we note that the quantum enhancement predicted via LHA−LSC for k_s and k_{as} does not coincide with any of the QCFs, and falls between the Schofield and harmonic/Schofield QCFs (cf. Table 3).

C. CO_2 in Liquid Neon at $\rho = 42.24$ nm^{-}3 and $T = 37.6$ K. The VER rate constants k_{as}, k_s, and k_{ivr} for the CO_2/Ne system are shown in Figure 7, as a function of frequency (on a semilog plot). The results obtained via the LHA−LSC method and fully classical calculations are shown. The values of k_{as}, k_s, and k_{ivr} at the actual frequencies ω_{as}, ω_s, and ω_{ivr} of the CO_2 molecule are given in Table 4. Also given in this table are the values

TABLE 3: k_{as}, k_s, and k_{ivr} in the CO_2/Ar System, as Obtained via the LHA−LSC Method[a]

CO_2/Ar	k_{as}/s^{-1} U	k_s/s^{-1} U	k_s/s^{-1} U + T	k_{ivr}/s^{-1} U
classical	$(6.5 \pm 1) \times 10^{-15}$	$(13 \pm 1) \times 10^{-2}$	$(14.1 \pm 1) \times 10^{-2}$	$(117 \pm 4) \times 10^{-4}$
nonclassical sampling	$(4 \pm 2) \times 10^{-9}$	$(17 \pm 3) \times 10^{1}$	$(17 \pm 3) \times 10^{1}$	$(6 \pm 1) \times 10^{-1}$
LHA−LSC	$(4 \pm 1) \times 10^{-7}$	$(11 \pm 1) \times 10^{2}$	$(11 \pm 1) \times 10^{2}$	$(6 \pm 1) \times 10^{-1}$
$f_{LHA-LSC}$	5.7×10^{7}	9×10^{3}	8×10^{3}	48
f_{St}	2	2	2	2
f_{H}	37	19	19	18
f_{Sc}	9.3×10^{7}	1.45×10^{5}	1.45×10^{5}	6.4×10^{3}
f_{MHS}	5.8×10^{5}	5×10^{2}	5×10^{2}	3×10^{2}

[a] See footnote *a* below Table 2.

TABLE 4: k_{as}, k_s, and k_{ivr} in the CO_2/Ne System, as Obtained via the LHA−LSC Method[a]

CO_2/Ne	k_{as}/s^{-1} U	k_s/s^{-1} U	k_s/s^{-1} U + T	k_{ivr}/s^{-1} U
classical	$(24 \pm 8) \times 10^{-20}$	$(5 \pm 1) \times 10^{-4}$	$(5 \pm 1) \times 10^{-4}$	$(99 \pm 8) \times 10^{-6}$
nonclassical sampling	$(6 \pm 2) \times 10^{-7}$	$(30 \pm 6) \times 10^{1}$	$(38 \pm 7) \times 10^{1}$	2.6 ± 0.4
LHA−LSC	$(15 \pm 4) \times 10^{-5}$	$(9 \pm 1) \times 10^{3}$	$(10 \pm 2) \times 10^{3}$	2.6 ± 0.4
$f_{LHA-LSC}$	6×10^{14}	1.9×10^{7}	2.4×10^{7}	2.6×10^{4}
f_{St}	2	2	2	2
f_{H}	92	48	48	44
f_{Sc}	9×10^{19}	2.6×10^{10}	2.6×10^{10}	3.4×10^{9}
f_{MHS}	9×10^{10}	1.1×10^{6}	1.1×10^{6}	4×10^{5}

[a] See footnote *a* below Table 2.

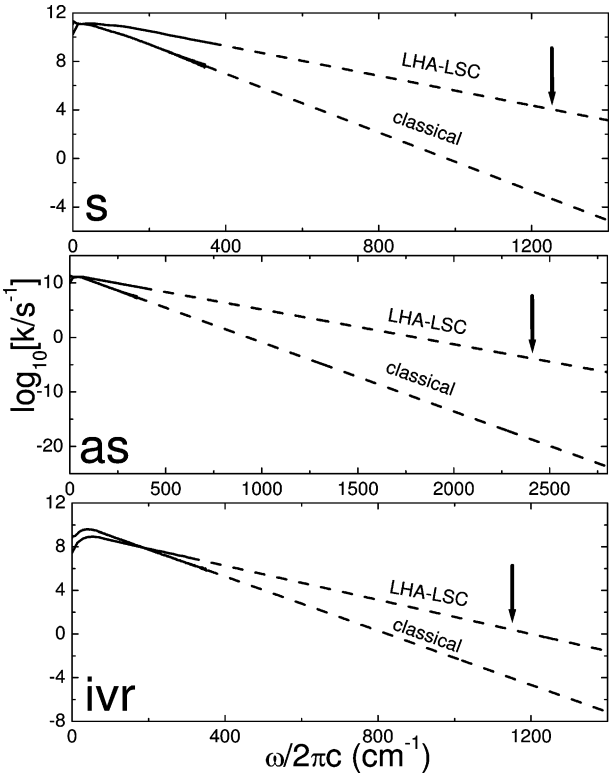

Figure 7. The classical and LHA−LSC frequency-dependent rate constants for the symmetric stretch, asymmetric stretch, and IVR, for CO_2 in neon. Calculated data are shown as solid lines. The dashed lines represent extrapolations to the corresponding frequencies of the symmetric and asymmetric stretches. The relevant frequencies are indicated by arrows.

predicted by only using nonclassical initial sampling, while neglecting the nonlocal terms.

The classical rate for direct VER of the asymmetric stretch in this system is even slower than in CO_2/Ar ($k_{as} \sim 10^{-19}$ s^{-1}), which can be attributed to the fact that $\beta\hbar\omega_{as} \sim 92$. Thus, the possibility of direct VER of the asymmetric stretch to the ground state can be ruled out. This remains true even if one takes into account the enhancement by 15 orders of magnitude of k_{as} predicted by the LHA−LSC method.

Similarly to the CO_2/Ar system, the fastest VER rate in this system corresponds to k_s. In this case, the LHA−LSC method predicts $k_s \sim 10^4$ s^{-1}, which represents a quantum enhancement by 7 orders of magnitude relative to the corresponding classical result ($\sim 5 \times 10^{-4}$ s^{-1}). The IVR rate is significantly slower than that of direct VER from the symmetric stretch ($k_{ivr} \sim 3$ s^{-1}), with a smaller, 4 orders of magnitude, quantum enhancement. Thus, the rate of VER from the excited asymmetric stretch is dictated by k_{ivr}, while that from the excited symmetric stretch is dictated by by k_s (and is therefore significantly faster). As for the CO_2/Ar system, the quantum enhancement predicted via LHA−LSC for k_s and k_{as} in the CO_2/Ne system is different from that predicted by various QCFs, and falls between the Schofield and harmonic/Schofield QCFs (cf. Table 4).

Finally, it is interesting to note a trend reversal in the VER rates between argon and neon as we go from the classical treatment to its semiclassical counterpart (cf. Tables 3 and 4). More specifically, while the classical VER rates in argon are *faster* than those in neon, the LHA−LSC-based VER rates are actually *slower* in argon than they are in neon. This implies that the reduction of the VER rates due to the lower temperature of the CO_2/Ne system is more than compensated for by a considerably larger quantum enhancement. This may be explained by the fact that neon has a smaller mass than argon and that the Ne−O interaction potential is somewhat softer than the Ar−O interaction potential, in the repulsive region. The CO_2/Ne system can therefore better penetrate classically forbidden areas on the repulsive region of the interaction potential, which would give rise to a larger quantum enhancement.

VIII. Summary

In this paper, we have extended the applicability range of the LHA−LSC method to the case of VER in polyatomic molecules in liquid solution. Although our model of choice is a relatively simple one, namely, a rigid, linear and symmetrical triatomic solute in a monatomic liquid, it already includes the main feature of VER in polyatomic systems, namely, the multiplicity of VER pathways. Our main conclusions, which we believe would also be relevant to many other polyatomic systems, can be summarized as follows:

1. Generally speaking, the LHA−LSC method predicts faster VER and IVR rates in comparison to the classical treatment.

2. The actual rate enhancement may be strongly pathway-dependent. For example, for the model studied here, the enhancement of intermolecular VER was found to be stronger than that of IVR.

3. A classical treatment may provide an incorrect prediction regarding the dependence of VER rates on the solvent. The example of CO_2 in argon and neon, where the classical VER rates are faster in the former, while the LHA−LSC-based VER rates are faster in the latter, demonstrates this point.

The next step is clearly to extend the methodology to more realistic models, and incorporate such important aspects as stretch-to-bend VER pathways, higher order IVR processes, nonlinear molecular geometries, and polar solute−solvent interactions. The investigation of these issues is currently underway in our group, and will be reported in future publications.

Acknowledgment. The authors are grateful for financial support from the National Science Foundation through Grant CHE-0306695.

Appendix: Useful Expressions for Calculating the LHA−LSC VER Rates

In this Appendix, we provide some technical details associated with the calculation of $C_s(t)$, $C_{as}(t)$, and $C_{ivr}(t)$ via the LHA−LSC method. The following notations and conventions are used throughout:

(1) The triatomic sites *a*, *b*, and *c* are labeled 3, 1, and 2, respectively.

(2) $\bar{\beta} = 5 - \beta$, such that $\beta = 2 \rightarrow \bar{\beta} = 3$ and $\beta = 3 \rightarrow \bar{\beta} = 2$ (it should be noted that β is used here as an index, and should not be confused with $\beta = 1/k_B T$).

(3) $\mathbf{r} = \mathbf{r}^{(i,0\beta)}$ corresponds to the vector pointing from the β site of the triatomic molecule to the *i*th solvent atom. $x = x^{(i,0\beta)}$, $y = y^{(i,0\beta)}$, and $z = z^{(i,0\beta)}$ correspond to the *x*, *y*, and *z* coordinates of this vector, and $r = |\mathbf{r}|$ corresponds to its length.

(4) $\bar{\mathbf{r}} = \mathbf{r}^{(i,0\bar{\beta})}$ corresponds to the vector pointing from the $\bar{\beta}$ site of the triatomic molecule to the *i*th solvent atom. $\bar{x} = x^{(i,0\bar{\beta})}$, $\bar{y} = y^{(i,0\bar{\beta})}$, and $\bar{z} = z^{(i,0\bar{\beta})}$ correspond to the *x*, *y*, and *z* coordinates of this vector, and $\bar{r} = |\bar{\mathbf{r}}|$ corresponds to its length.

(5) The elements of the transformation matrix from local to normal mode coordinates:

$$\eta_s^{(1)} = 0, \quad \eta_s^{(2)} = \frac{1}{\sqrt{2m_A}}, \quad \eta_s^{(3)} = -\frac{1}{\sqrt{2m_A}}$$

$$\eta_{as}^{(1)} = -\sqrt{\frac{2m_A}{Mm_B}}, \quad \eta_{as}^{(2)} = \eta_{as}^{(3)} = \sqrt{\frac{m_B}{2m_A M}} \qquad \text{(A1)}$$

(6) Various combinations of the pair potential functions and their derivatives:

$$\Phi_4 \equiv r\Phi_3'(r) - 2(4-1)\Phi_3(r) = r^4\phi'''' - 6r^3\phi''' + 15r^2\phi'' - 15r\phi' = \bar{w}(r) \qquad \text{(A2)}$$

$$\Phi_3 \equiv r\Phi_2'(r) - 2(3-1)\Phi_2(r) = r^3\phi''' - 3r^2\phi'' + 3r\phi' = w(r) \qquad \text{(A3)}$$

$$\Phi_2 \equiv r\Phi_1'(r) - 2(2-1)\Phi_1(r) = r^2\phi'' - r\phi' = v(r) \qquad \text{(A4)}$$

$$\Phi_1 \equiv r\Phi_0' - 2(1-1)\Phi_0 = r\phi' = l(r) \qquad \text{(A5)}$$

$$\Phi_0 \equiv \phi(r) \qquad \text{(A6)}$$

It should be noted that $\phi(r)$ is one of three pair potentials. The specific choice is dictated by the two sites involved in defining the distance *r*.

The LHA requires the calculation of the first and second derivatives of the potential energy with respect to the Cartesian coordinates of the atoms. Explicit expressions for these derivatives in the case of a diatomic molecule in a monatomic solvent were given in ref 55, where LJ pair potentials were also assumed. An extension of these results for the case of a linear triatomic solute is rather straightforward and will therefore not be reproduced here.

We next consider the calculation of the quantum nonlocal terms $\{D_{U,n}\}$ where $n = a, as$. The explicit expressions for these terms are given in ref 54. As shown there, calculating the real part of $\{D_{U,n}\}$ requires knowledge of the second derivatives of $F_{U,n}$ with respect to the atomic coordinates. Explicit expressions of those derivatives are given below.

We first consider the case where the derivative is with respect to coordinates of atoms in the triatomic molecule:

$$\frac{\partial^2 F_{U,n}}{\partial x^{(0\beta)}\,\partial x^{(0\beta)}} = \sum_{i=1}^{N_{Ar}} \eta_n^{(\beta)} \left\{ \frac{w(r)x^2 + v(r)r^2}{r^6}\mathbf{r}\cdot\Omega + 2v(r)\frac{x\Omega_x}{r^4} \right\}; \quad \text{for } \beta = 1 \qquad \text{(A7)}$$

$$\frac{\partial^2 F_{U,n}}{\partial x^{(0\beta)}\,\partial x^{(0\beta)}} = \sum_{i=1}^{N_{Ar}} \eta_n^{(\beta)} \left\{ \frac{w(r)x^2 + v(r)r^2}{r^6}\mathbf{r}\cdot\Omega + 2v(r)\frac{x\Omega_x}{r^4} \mp \frac{v(r)x^2 + l(r)r^2}{r^4 r_e} \right\}; \quad \text{for } \beta = 2, 3 \qquad \text{(A8)}$$

Here, as in the rest of the paper, $\mp \rightarrow -$ for $\beta = 2$ and $\mp \rightarrow +$ for $\beta = 3$ ($\pm \rightarrow +$ for $\beta = 2$ and $\pm \rightarrow -$ for $\beta = 3$).

$$\frac{\partial^2 F_{U,n}}{\partial x^{(0\beta)}\,\partial y^{(0\beta)}} = \sum_{i=1}^{N_{Ar}} \eta_n^{(\beta)} \left\{ \frac{w(r)xy}{r^6}\mathbf{r}\cdot\Omega + v(r)\frac{x\Omega_y + y\Omega_x}{r^4} \right\}; \quad \text{for } \beta = 1 \qquad \text{(A9)}$$

$$\frac{\partial^2 F_{U,n}}{\partial x^{(0\beta)}\,\partial y^{(0\beta)}} = \sum_{i=1}^{N_{Ar}} \eta_n^{(\beta)} \left\{ \frac{w(r)xy}{r^6}\mathbf{r}\cdot\Omega + v(r)\frac{x\Omega_y + y\Omega_x}{r^4} \mp \frac{v(r)xy}{r^4 r_e} \right\}; \quad \text{for } \beta = 2, 3 \qquad \text{(A10)}$$

$$\frac{\partial^2 F_{U,n}}{\partial x^{(0\beta)}\,\partial x^{(0\bar{\beta})}} = \pm\sum_{i=1}^{N_{Ar}}\left\{\eta_n^{(\beta)}\frac{v(r)x^2 + l(r)r^2}{2r^4 r_e} - \eta_n^{(\bar{\beta})}\frac{v(\bar{r})\bar{x}^2 + l(\bar{r})\bar{r}^2}{2\bar{r}^4 r_e}\right\}; \quad \text{for } \beta = 2, 3 \tag{A11}$$

$$\frac{\partial^2 F_{U,n}}{\partial x^{(0\beta)}\,\partial x^{(01)}} = \mp\sum_{i=1}^{N_{Ar}}\eta_n^{(1)}\left\{\frac{v(r)x^2 + l(r)r^2}{2r^4 r_e}\right\}; \quad \text{for } \beta = 2, 3 \tag{A12}$$

Here, as well as throughout the remainder of this Appendix, expressions for other second derivatives can be obtained by substituting x and y by other combinations of coordinates.

$$\frac{\partial^2 F_{U,n}}{\partial x^{(0\beta)}\,\partial y^{(0\bar{\beta})}} = \pm\sum_{i=1}^{N_{Ar}}\left\{\eta_n^{(\beta)}\frac{v(r)xy}{2r^4 r_e} - \eta_n^{(\bar{\beta})}\frac{v(\bar{r})\bar{x}\bar{y}}{2\bar{r}^4 r_e}\right\}; \quad \text{for } \beta = 2, 3 \tag{A13}$$

$$\frac{\partial^2 F_{U,n}}{\partial x^{(0\beta)}\,\partial y^{(01)}} = \mp\sum_{i=1}^{N_{Ar}}\eta_n^{(1)}\left\{\frac{v(r)xy}{2r^4 r_e}\right\}; \quad \text{for } \beta = 2, 3 \tag{A14}$$

We next consider the case of a mixed second derivative with respect to the solvent atom and triatomic site coordinates:

$$\frac{\partial^2 F_{U,n}}{\partial x^{(i)}\,\partial x^{(0\beta)}} = -\eta_n^{(1)}\left\{\frac{w(r)x^2 + v(r)r^2}{r^6}\mathbf{r}\cdot\Omega + 2v(r)\frac{x\Omega_x}{r^4}\right\}; \quad \text{for } \beta = 1 \tag{A15}$$

$$\frac{\partial^2 F_{U,n}}{\partial x^{(i)}\,\partial x^{(0\beta)}} = -\eta_n^{(\beta)}\left\{\frac{w(r)x^2 + v(r)r^2}{r^6}\mathbf{r}\cdot\Omega + 2v(r)\frac{x\Omega_x}{r^4}\right\} \pm \sum_{\beta=1}^{3}\eta_n^{(\beta)}\frac{v(r)x^2 + l(r)r^2}{2r^4 r_e}; \quad \text{for } \beta = 2, 3 \tag{A16}$$

$$\frac{\partial^2 F_{U,n}}{\partial x^{(i)}\,\partial y^{(0\beta)}} = -\eta_n^{(1)}\left\{\frac{w(r)xy}{r^6}\mathbf{r}\cdot\Omega + v(r)\frac{x\Omega_y + y\Omega_x}{r^4}\right\}; \quad \text{for } \beta = 1 \tag{A17}$$

$$\frac{\partial^2 F_{U,n}}{\partial x^{(i)}\,\partial y^{(0\beta)}} = -\eta_n^{(\beta)}\left\{\frac{w(r)xy}{r^6}\mathbf{r}\cdot\Omega + v(r)\frac{x\Omega_y + y\Omega_x}{r^4}\right\} \pm \sum_{\beta=1}^{3}\eta_n^{(\beta)}\frac{v(r)xy}{2r^4 r_e}; \quad \text{for } \beta = 2, 3 \tag{A18}$$

Finally, we consider the case of a second derivative with respect to a solvent atom coordinate:

$$\frac{\partial^2 F_{U,n}}{\partial x^{(i)}\,\partial x^{(i)}} = \sum_{\beta=1}^{3}\eta_n^{(\beta)}\left[\frac{w(r)x^2 + v(r)r^2}{r^6}\mathbf{r}\cdot\Omega + 2v(r)\frac{x\Omega_x}{r^4}\right] \tag{A19}$$

$$\frac{\partial^2 F_{U,n}}{\partial x^{(i)}\,\partial y^{(i)}} = \sum_{\beta=1}^{3}\eta_n^{(\beta)}\left[\frac{w(r)xy}{r^6}\mathbf{r}\cdot\Omega + v(r)\frac{x\Omega_y + y\Omega_x}{r^4}\right] \tag{A20}$$

$$\frac{\partial^2 F_{U,n}}{\partial x^{(i)}\,\partial x^{(j)}} = \frac{\partial^2 F_{U,n}}{\partial x^{(i)}\,\partial y^{(j)}} = 0; \quad \text{for } i \neq j \tag{A21}$$

We next consider the calculation of the quantum nonlocal term $D_{U,s,as}$. Calculating the real part of this term requires knowledge of the second derivative of $G_{aa} \equiv G_{33}$ and $G_{cc} \equiv G_{22}$ with respect to the atomic coordinates (cf. eq 20). Explicit expressions of those derivatives are given below. We first consider the case where the derivative is with respect to coordinates of atoms in the triatomic molecule:

$$\frac{\partial^2 G_{\beta\beta}}{\partial x^{(0\beta)}\,\partial x^{(0\beta)}} = \sum_{i=1}^{N_{Ar}}\left\{\frac{\bar{w}(r)x^2 + w(r)r^2}{r^8}(\mathbf{r}\cdot\Omega)^2 + 4\frac{w(r)}{r^6}\left(x\Omega_x \mp \frac{x^2}{2r_e}\right)\mathbf{r}\cdot\Omega + 2\frac{v(r)}{r^4}\left[\left(\frac{x}{2r_e} \mp \Omega_x\right)^2 \mp \frac{1}{r_e}\mathbf{r}\cdot\Omega\right] + \frac{w(r)x^2}{r^6} + \frac{v(r)}{r^4}\right\}; \quad \text{for } \beta = 2, 3 \tag{A22}$$

$$\frac{\partial^2 G_{\beta\beta}}{\partial x^{(0\bar{\beta})}\,\partial x^{(0\beta)}} = \sum_{i=1}^{N_{Ar}}\left\{\pm\frac{w(r)x^2 + v(r)r^2}{r_e r^6}\mathbf{r}\cdot\Omega \pm \frac{v(r)}{r_e r^4}\Omega_x x - \frac{v(r)x^2}{2r_e^2 r^4}\right\}; \quad \text{for } \beta = 2, 3 \tag{A23}$$

$$\frac{\partial^2 G_{\beta\beta}}{\partial x^{(0\bar{\beta})}\,\partial x^{(0\bar{\beta})}} = \sum_{i=1}^{N_{Ar}}\left\{\frac{v(r)x^2}{2r_e^2 r^4}\right\}; \quad \text{for } \beta = 2, 3 \tag{A24}$$

$$\frac{\partial^2 G_{\beta\beta}}{\partial y^{(0\beta)}\,\partial x^{(0\beta)}} = \sum_{i=1}^{N_{Ar}}\left\{\frac{\bar{w}(r)xy}{r^8}(\mathbf{r}\cdot\Omega)^2 + 2\frac{w(r)}{r^6}(x\Omega_y + y\Omega_x)\mathbf{r}\cdot\Omega \mp 2\frac{w(r)xy}{r_e r^6}\mathbf{r}\cdot\Omega + 2\frac{v(r)}{r^4}\left(\frac{x}{2r_e} \mp \Omega_x\right)\left(\frac{y}{2r_e} \mp \Omega_y\right) + \frac{w(r)xy}{r^6}\right\}; \quad \text{for } \beta = 2, 3 \tag{A25}$$

$$\frac{\partial^2 G_{\beta\beta}}{\partial y^{(0\bar{\beta})}\,\partial x^{(0\beta)}} = \sum_{i=1}^{N_{Ar}}\left\{\pm\frac{w(r)xy}{r_e r^6}\mathbf{r}\cdot\Omega \pm \frac{v(r)}{r_e r^4}\Omega_x y - \frac{v(r)xy}{2r_e^2 r^4}\right\}; \quad \text{for } \beta = 2, 3 \tag{A26}$$

$$\frac{\partial^2 G_{\beta\beta}}{\partial y^{(0\bar{\beta})}\,\partial x^{(0\bar{\beta})}} = \sum_{i=1}^{N_{Ar}}\left\{\frac{v(r)xy}{2r_e^2 r^4}\right\}; \quad \text{for } \beta = 2, 3 \tag{A27}$$

$$\frac{\partial^2 G_{\beta\beta}}{\partial x^{(01)}\,\partial x^{(0\beta')}} = \frac{\partial^2 G_{\beta\beta}}{\partial y^{(01)}\,\partial x^{(0\beta')}} = 0; \quad \text{for } \beta' = 1, 2, 3 \tag{A28}$$

We next consider the case of a mixed second derivative with respect to the solvent atom and triatomic site coordinates:

$$\frac{\partial^2 G_{\beta\beta}}{\partial x^{(i)}\,\partial x^{(0\beta)}} = -\frac{\bar{w}(r)x^2 + w(r)r^2}{r^8}(\mathbf{r}\cdot\Omega)^2 - 4\frac{w(r)}{r^6}x\Omega_x\mathbf{r}\cdot\Omega \pm \frac{w(r)x^2}{r_e r^6}\mathbf{r}\cdot\Omega \pm 2\frac{v(r)}{r^4}\left[\left(\frac{x}{2r_e} \mp \Omega_x\right)\Omega_x + \frac{1}{2r_e}\mathbf{r}\cdot\Omega\right] - \frac{w(r)x^2}{r^6} - \frac{v(r)}{r^4}; \quad \text{for } \beta = 2, 3 \quad \text{(A29)}$$

$$\frac{\partial^2 G_{\beta\beta}}{\partial x^{(i)}\,\partial x^{(0\bar{\beta})}} = \mp\frac{w(r)x^2 + v(r)r^2}{r_e r^6}\mathbf{r}\cdot\Omega \mp \frac{v(r)}{r_e r^4}\Omega_x x; \quad \text{for } \beta = 2, 3 \quad \text{(A30)}$$

$$\frac{\partial^2 G_{\beta\beta}}{\partial y^{(i)}\,\partial x^{(0\beta)}} = -\frac{\bar{w}(r)xy}{r^8}(\mathbf{r}\cdot\Omega)^2 - 2\frac{w(r)}{r^6}(x\Omega_y + y\Omega_x)\mathbf{r}\cdot\Omega \pm \frac{w(r)xy}{r_e r^6}\mathbf{r}\cdot\Omega \pm 2\frac{v(r)}{r^4}\left(\frac{x}{2r_e} \mp \Omega_x\right)\Omega_y - \frac{w(r)xy}{r^6}; \quad \text{for } \beta = 2, 3 \quad \text{(A31)}$$

$$\frac{\partial^2 G_{\beta\beta}}{\partial y^{(i)}\,\partial x^{(0\bar{\beta})}} = \mp\frac{w(r)xy}{r_e r^6}\mathbf{r}\cdot\Omega \mp \frac{v(r)}{r_e r^4}x\Omega_y; \quad \text{for } \beta = 2, 3 \quad \text{(A32)}$$

$$\frac{\partial^2 G_{\beta\beta}}{\partial x^{(i)}\,\partial x^{(01)}} = \frac{\partial^2 G_{\beta\beta}}{\partial y^{(i)}\,\partial x^{(01)}} = 0; \quad \text{for } \beta = 2, 3 \quad \text{(A33)}$$

Finally, we consider the case of a second derivative with respect to a solvent atom coordinate:

$$\frac{\partial^2 G_{\beta\beta}}{\partial x^{(i)}\,\partial x^{(i)}} = \frac{\bar{w}(r)x^2 + w(r)r^2}{r^8}(\mathbf{r}\cdot\Omega)^2 + 4\frac{w(r)}{r^6}x\Omega_x\mathbf{r}\cdot\Omega + 2\frac{v(r)}{r^4}\Omega_x{}^2 + \frac{w(r)x^2}{r^6} + \frac{v(r)}{r^4} \quad \text{for } \beta = 2, 3 \quad \text{(A34)}$$

$$\frac{\partial^2 G_{\beta\beta}}{\partial y^{(i)}\,\partial x^{(i)}} = \frac{\bar{w}(r)xy}{r^8}(\mathbf{r}\cdot\Omega)^2 + 2\frac{w(r)}{r^6}(x\Omega_y + y\Omega_x)\mathbf{r}\cdot\Omega + 2\frac{v(r)}{r^4}\Omega_x\Omega_y + \frac{w(r)xy}{r^6}; \quad \text{for } \beta = 2, 3 \quad \text{(A35)}$$

$$\frac{\partial^2 G_{\beta\beta}}{\partial x^{(i)}\,\partial x^{(j)}} = \frac{\partial^2 G_{\beta\beta}}{\partial x^{(i)}\,\partial y^{(j)}} = 0; \quad \text{for } \beta = 2, 3, \text{ and } i \neq j \quad \text{(A36)}$$

References and Notes

(1) Faltermeier, B.; Protz, R.; Maier, M. *Chem. Phys.* **1981**, *62*, 377.
(2) Brueck, S. R. J.; Osgood, R. M. *Chem. Phys. Lett.* **1976**, *39*, 568.
(3) Oxtoby, D. W. *Adv. Chem. Phys.* **1981**, *47* (Part 2), 487.
(4) Chateau, M.; et al. *J. Chem. Phys.* **1979**, *71*, 4799.
(5) Delalande, C.; Gale, G. M. *J. Chem. Phys.* **1979**, *71*, 4804.
(6) Delalande, C.; Gale, G. M. *J. Chem. Phys.* **1980**, *73*, 1918.
(7) Faltermeier, B.; Protz, R.; Maier, M.; Werner, E. *Chem. Phys. Lett.* **1980**, *74*, 425.
(8) Oxtoby, D. W. *Annu. Rev. Phys. Chem.* **1981**, *32*, 77.
(9) Oxtoby, D. W. *J. Phys. Chem.* **1983**, *87*, 3028.
(10) Chesnoy, J.; Gale, G. M. *Ann. Phys. Fr.* **1984**, *9*, 893.
(11) Chesnoy, J.; Gale, G. M. *Adv. Chem. Phys.* **1988**, *70* (Part 2), 297.
(12) Harris, C. B.; Smith, D. E.; Russell, D. J. *Chem. Rev.* **1990**, *90*, 481.
(13) Miller, D. W.; Adelman, S. A. *Int. Rev. Phys. Chem.* **1994**, *13*, 359.
(14) Stratt, R. M.; Maroncelli, M. *J. Phys. Chem.* **1996**, *100*, 12981.
(15) Owrutsky, J. C.; Raftery, D.; Hochstrasser, R. M. *Annu. Rev. Phys. Chem.* **1994**, *45*, 519.
(16) Elsaesser, T.; Kaiser, W. *Annu. Rev. Phys. Chem.* **1991**, *42*, 83.
(17) Calaway, W. F.; Ewing, G. E. *J. Chem. Phys.* **1975**, *63*, 2842.
(18) Laubereau, A.; Kaiser, W. *Rev. Mod. Phys.* **1978**, *50*, 607.
(19) Roussignol, P.; Delalande, C.; Gale, G. M. *Chem. Phys.* **1982**, *70*, 319.
(20) Heilweil, E. J.; Doany, F. E.; Moore, R.; Hochstrasser, R. M. *J. Chem. Phys.* **1982**, *76*, 5632.
(21) Heilweil, E. J.; Casassa, M. P.; Cavanagh, R. R.; Stephenson, J. C. *Chem. Phys. Lett.* **1985**, *117*, 185.
(22) Heilweil, E. J.; Casassa, M. P.; Cavanagh, R. R.; Stephenson, J. C. *J. Chem. Phys.* **1986**, *85*, 5004.
(23) Harris, A. L.; Brown, J. K.; Harris, C. B. *Annu. Rev. Phys. Chem* **1988**, *39*, 341.
(24) Paige, M. E.; Russell, D. J.; Harris, C. B. *J. Chem. Phys.* **1986**, *85*, 3699.
(25) Owrutsky, J. C.; et al. *Chem. Phys. Lett.* **1991**, *184*, 368.
(26) Moustakas, A.; Weitz, E. *J. Chem. Phys.* **1993**, *98*, 6947.
(27) Kliner, D. A. V.; Alfano, J. C.; Barbara, P. F. *J. Chem. Phys.* **1993**, *98*, 5375.
(28) Zimdars, D.; et al. *Phys. Rev. Lett.* **1993**, *70*, 2718.
(29) Pugliano, N.; Szarka, A. Z.; Gnanakaran, S.; Hochstrasser, R. M. *J. Chem. Phys.* **1995**, *103*, 6498.
(30) Paige, M. E.; Harris, C. B. *Chem. Phys.* **1990**, *149*, 37.
(31) Salloum, A.; Dubost, H. *Chem. Phys.* **1994**, *189*, 179.
(32) Tokmakoff, A.; Sauter, B.; Fayer, M. D. *J. Chem. Phys.* **1994**, *100*, 9035.
(33) Tokmakoff, A.; Fayer, M. D. *J. Chem. Phys.* **1995**, *103*, 2810.
(34) Urdahl, R. S.; et al. *J. Chem. Phys.* **1997**, *107*, 3747.
(35) Owrutsky, J. C.; Li, M.; Locke, B.; Hochstrasser, R. M. *J. Phys. Chem.* **1995**, *99*, 4842.
(36) Laenen, R.; Rauscher, C.; Laubereau, A. *Phys. Rev. Lett.* **1998**, *80*, 2622.
(37) Woutersen, S.; Emmerichs, U.; Nienhuys, H.; Bakker, H. J. *Phys. Rev. Lett.* **1998**, *81*, 1106.
(38) Myers, D. J.; Urdahl, R. S.; Cherayil, B. J.; Fayer, M. D. *J. Chem. Phys.* **1997**, *107*, 9741.
(39) Myers, D. J.; et al. *J. Chem. Phys.* **1998**, *109*, 5971.
(40) Sagnella, D. E.; et al. *Proc. Natl. Acad. Sci. U.S.A.* **1999**, *96*, 14324.
(41) Hamm, P.; Lim, M.; Hochstrasser, R. M. *J. Chem. Phys.* **1997**, *107*, 1523.
(42) Lawrence, C. P.; Skinner, J. L. *J. Chem. Phys.* **2002**, *117*, 5827.
(43) Deng, Y.; Stratt, R. M. *J. Chem. Phys.* **2002**, *117*, 1735.
(44) Deng, Y.; Stratt, R. M. *J. Chem. Phys.* **2002**, *117*, 10752.
(45) Sibert, E. L., III; Rey, R. *J. Chem. Phys.* **2002**, *116*, 237.
(46) Li, S.; Thompson, W. H. *J. Chem. Phys.* **2003**, *107*, 8696.
(47) Bakker, H. J. *J. Chem. Phys.* **2004**, *121*, 10088.
(48) Gulmen, T. S.; Sibert, E. L., III. *J. Phys. Chem. A* **2004**, *108*, 2389.
(49) Gulmen, T. S.; Sibert, E. L., III. *J. Phys. Chem. A* **2005**, *109*, 5777.
(50) Zwanzig, R. *J. Chem. Phys.* **1961**, *34*, 1931.
(51) Everitt, K. F.; Egorov, S. A.; Skinner, J. L. *Chem. Phys.* **1998**, *235*, 115.
(52) Everitt, K. F.; Skinner, J. L. *J. Chem. Phys.* **1999**, *110*, 4467.
(53) Shi, Q.; Geva, E. *J. Phys. Chem. A* **2003**, *107*, 9059.
(54) Shi, Q.; Geva, E. *J. Phys. Chem. A* **2003**, *107*, 9070.
(55) Ka, B. J.; Shi, Q.; Geva, E. *J. Phys. Chem. A* **2005**, *109*, 5527.
(56) Berne, B. J.; Jortner, J.; Gordon, R. *J. Chem. Phys.* **1967**, *47*, 1600.
(57) Bader, J. S.; Berne, B. J. *J. Chem. Phys.* **1994**, *100*, 8359.
(58) Egorov, S. A.; Everitt, K. F.; Skinner, J. L. *J. Phys. Chem. A* **1999**, *103*, 9494.
(59) Egorov, S. A.; Skinner, J. L. *J. Chem. Phys.* **2000**, *112*, 275.
(60) Skinner, J. L.; Park, K. *J. Phys. Chem. B* **2001**, *105*, 6716.
(61) Rostkier-Edelstein, D.; Graf, P.; Nitzan, A. *J. Chem. Phys.* **1997**, *107*, 10470.
(62) Rostkier-Edelstein, D.; Graf, P.; Nitzan, A. *J. Chem. Phys.* **1998**, *108*, 9598.
(63) Everitt, K. F.; Skinner, J. L.; Ladanyi, B. M. *J. Chem. Phys.* **2002**, *116*, 179.
(64) Berens, P. H.; White, S. R.; Wilson, K. R. *J. Chem. Phys.* **1981**, *75*, 515.
(65) Frommhold, L. *Collision-induced absorption in gases*, Vol. 2 of *Cambridge Monographs on Atomic, Molecular, and Chemical Physics*, 1st ed.; Cambridge University Press: Cambridge, England, 1993.
(66) Skinner, J. L. *J. Chem. Phys.* **1997**, *107*, 8717.
(67) An, S. C.; Montrose, C. J.; Litovitz, T. A. *J. Chem. Phys.* **1967**, *64*, 3717.
(68) Egorov, S. A.; Skinner, J. L. *Chem. Phys. Lett.* **1998**, *293*, 439.
(69) Schofield, P. *Phys. Rev. Lett.* **1960**, *4*, 239.
(70) Egelstaff, P. A. *Adv. Phys.* **1962**, *11*, 203.
(71) Kneller, G. R. *Mol. Phys.* **1994**, *83*, 63.
(72) Shi, Q.; Geva, E. *J. Chem. Phys.* **2003**, *118*, 8173.
(73) Graener, H.; Seifert, G.; Laubereau, A. *Phys. Rev. Lett.* **1991**, *66*, 2092.
(74) Vodopyanov, K. L. *J. Chem. Phys.* **1991**, *94*, 5389.
(75) Nienhuys, H.; Woutersen, S.; van Santen, R. A.; Bakker, H. J. *J. Chem. Phys.* **1900**, *111*, 1494.

(76) Deak, J. C.; Rhea, S. T.; Iwaki, L. K.; Dlott, D. D. *J. Phys. Chem. A* **2000**, *104*, 4866.
(77) Rey, R.; Hynes, J. T. *Chem. Rev.* **2004**, *104*, 1915.
(78) Bakker, H. J.; *J. Chem. Phys.* **1993**, *98*, 8496.
(79) Deak, J. C.; Iwaki, L. K.; Rhea, S. T.; Dlott, D. D. *J. Raman Spectrosc.* **2000**, *31*, 263.
(80) Dlott, D. D. *Chem. Phys.* **2001**, *266*, 149.
(81) Hofmann, M.; Graener, H. *Chem. Phys.* **1996**, *206*, 129.
(82) Graener, H.; Zürl, R.; Hofmann, M. *J. Phys. Chem. B* **1997**, *101*, 1745.
(83) Seifert, G.; Zürl, R.; Graener, H. *J. Phys. Chem. A* **1999**, *103*, 10749.
(84) Seifert, G.; Zürl, R.; Patzlaff, T.; Graener, H. *J. Chem. Phys.* **2000**, *112*, 6349.
(85) Deak, J. C.; Iwaki, L. K.; Dlott, D. D. *Chem. Phys. Lett.* **1998**, *293*, 405.
(86) Deak, J. C.; Iwaki, L. K.; Dlott, D. D. *J. Phys. Chem.* A **1998**, *102*, 8193.
(87) Iwaki, L. K.; Deak, J. D.; Rhea, S. T.; Dlott, D. D. *Chem. Phys. Lett.* **1999**, *303*, 176.
(88) Deak, J. C.; Iwaki, L. K.; Dlott, D. D. *J. Phys. Chem. A* **1999**, *103*, 971.
(89) Hayes, S. C.; Phipott, M. J.; Reid, P. J. *J. Chem. Phys.* **1998**, *109*, 2596.
(90) Wang, Z.; Pakoulev, A.; Pang, Y.; Dlott, D. D. *Chem. Phys. Lett.* **2003**, *378*, 281.
(91) Pakoulev, A.; Wang, Z.; Dlott, D. D. *Chem. Phys. Lett.* **2003**, *371*, 2203.
(92) Pakoulev, A.; Wang, Z.; Pang, Y.; Dlott, D. D. *Chem. Phys. Lett.* **2003**, *380*, 404.
(93) Wang, Z.; Pakoulev, A.; Pang, Y.; Dlott, D. D. *J. Phys. Chem. A* **2004**, *108*, 9054.
(94) Wang, Z.; Pang, Y.; Dlott, D. D. *Chem. Phys. Lett.* **2004**, *397*, 40.
(95) Iwaki, L. K.; Dlott, D. D. *Chem. Phys. Lett.* **2000**, *321*, 419.
(96) Iwaki, L. K.; Dlott, D. D. *J. Phys. Chem. A* **2000**, *104*, 9101.
(97) Wang, Z.; Pakoulev, A.; Dlott, D. D. *Science* **2002**, *296*, 2201.
(98) Chorny, I.; Vieceli, J.; Benjamin, I. *J. Chem. Phys.* **2002**, *116*, 8904.
(99) Rey, R.; Hynes, J. T. *J. Chem. Phys.* **1996**, *104*, 2356.
(100) Lawrence, C. P.; Skinner, J. L. *J. Chem. Phys.* **2003**, *119*, 1623.
(101) Ferrario, M.; Klein, M. L.; McDonald, I. R. *Chem. Phys. Lett.* **1993**, *213*, 537.
(102) Morita, A.; Kato, S. *J. Chem. Phys.* **1998**, *109*, 5511.
(103) Hillery, M.; O'Connell, R. F.; Scully, M. O.; Wigner, E. P. *Phys. Rep.* **1984**, *106*, 121.
(104) Allen, M. P.; Tildesley, D. J. *Computer Simulation of Liquids*; Clarendon: Oxford, 1987.
(105) Nitzan, A.; Mukamel, S.; Jortner, J. *J. Chem. Phys.* **1974**, *60*, 3929.
(106) Nitzan, A.; Mukamel, S.; Jortner, J. *J. Chem. Phys.* **1975**, *63*, 200.
(107) Jang, S.; Voth, G. A. *J. Chem. Phys.* **1997**, *107*, 9514.
(108) Press, W. H.; Flannery, B. P.; Teukolsky, S. A.; Vetterling, W. T. *Numerical Recipes*; Cambridge University Press: Cambridge, 1986.